

# Unsupervised low-light image enhancement using statistic modules and dense connections

Yunqi Ma<sup>1</sup> and Danwei Chen<sup>\*1</sup>

<sup>1</sup> Nanjing University of Post and Telecommunication, Nanjing, China  
chendw@njupt.edu.cn

**Abstract.** Low-light Image Enhancement (LLIE) is a crucial strategy for improving the brightness and visual characteristics of underexposed images. Traditional and machine learning-based LLIE methods often use a single image or map to merge the most prominent channel in RGB. However, these approaches presents challenges in achieving a comprehensive understanding of the image data due to the limited information available from a single source. Leveraging a single image or map may limit the algorithm's ability to capture the full spectrum of details and nuances present in the original image. Therefore, it is important to explore alternative approaches that can capture a more comprehensive and detailed representation of the input data. In this paper, we introduce an unsupervised approach, SDLLIE, which combines the advantages of retinex theory and deep learning. Firstly, a statistical module is used to extract various information from the input map, allowing for a comprehensive analysis of the image data. Secondly, dense connections are incorporated to prevent network degradation and facilitate the smooth flow of information across layers. Before extracting the illumination and reflectance components, we remove noise to improve the quality and accuracy of low-light images. To align the generated results with the desired outcomes, we use a set of customized loss functions to guide the training process and optimize the network parameters effectively. Our proposed SDLLIE method has been comprehensively evaluated using both quantitative and qualitative measures on three widely-recognized benchmark datasets. The results demonstrate its considerable performance when compared to existing state-of-the-art approaches.

**Keywords:** Retinex, Statistic, Dense Connection.

## 1 Introduction

Images that are acquired under lighting conditions that are not optimal frequently suffer from composite distortions, which include limited visibility, low contrast, and interference from the sensor. Those images with insufficient exposure are not suitable for signal processing as they pose difficulty for human visualization and various computer vision procedures. In order to uncover the hidden details that are present in the low-light image and to prevent the performance of follow-up visual tasks from deteriorating, boffins have put a significant amount of effort into optimizing contrast,

\*Corresponding author

restoring texture, and removing sensor noise for the low-light image. Especially for Low-light Image Enhancement(LLIE), a considerable number of algorithms have been presented over the course of the last few decades.

Histogram equalization based approaches and Retinex model based approaches are traditional LLIE methodologies. The former alters the pixel intensity distribution by shifting the values over the histogram, thereby boosting the contrast and enhancing the visual quality. The latter have been extensively used in the LLIE field due to Retinex theory, which is a good representation of human color perception. In Retinex theory, a picture  $I$  can be decomposed into lamination  $L$  and reflection spectrum  $R$  using the equation  $I = L \circ R$ , where  $\circ$  represents the element-by-element multiplication. Nevertheless, the conventional Retinex model, in its original form, does not account for the presence of noise, which is unavoidable in poor pictures. To that end, a noise item  $N$  introduced in the robust Retinex model [1].

As time goes by, LLIE algorithms have achieved considerable breakthroughs. For these methods, the majority of solutions are designed to utilize both low-level light and normal-level light image pairs [2]. However, capturing photos with varying lighting levels in the physical world situation is time-intensive and costly process [3]. To minimize the necessity for normal-light images, unsupervised and zero-shot LLIE techniques are proposed. However, the majority of self-supervised approaches rely on prior knowledge, which combines the highest score in the red, green and blue channels with the original three channels to provide direct training of the network. In a complicated natural environment, it is tough to produce better results utilizing these tactics. Furthermore, deepening the depth of ordinary convolution is likely to cause network degradation.

To handle the issue of prior knowledge and network degradation, we offer a general learning-based LLIE technique, entitled SDLLIE. The fundamental principle of our approach is to properly utilize information in underexposed images. Hence, we investigate leveraging the Deep learning methodologies and retinex theory to dissect poor-light images into lamination, reflectance and noise maps. To begin with, we utilize statistical approaches to enrich the input information. Second, in contrast to the Retinex decomposition method that was used previously, the noise is estimated and then deleted from the raw picture. The outcome of this process is used afterwards as an input for subsequent estimating operations. Finally, by effectively leveraging dense connections, we mitigate the issue of excessive information loss typically associated with deeper network architectures. As a result, the suggested SDLLIE obtains competing performance in publicly available LLIE datasets by utilizing a steady network and a few of efficient loss functions. In summary, the contributions of this paper are the following:

- We come up with a general LLIE method that just requires images in low light conditions. The neural network is built on Retinex decomposition with dense connections and a few important loss functions.
- In order to acquire a comprehensive understanding of underexposed images, we have incorporated a statistical module for refinement.
- We validate the presented approach on multiple publicly available datasets, and the outcomes of the experiments confirm its superior performance.

## 2 Related Work

Various LLIE approaches have been put forward over the past few decades, which can be categorised as traditional methods and learning-oriented approaches.

### 2.1 Traditional Approaches

Histogram Equalization is a technique for illuminating an image by expanding its dynamic range. For instance, Abdullah Al-Wadud et al. [4] employed gray-level allocation and segmented the picture histogram into many partial histograms. Celik and Tjahjadi [5] utilized contextual data modeling, which involves the application of a 2D histogram of an input picture to produce non-linear data mappings for creating aesthetically pleasing enhancements to different types of pictures. Liu et al. derived the required parameters to speed up computations.

Retinex-based approaches dissect underexposed images into reflectivity and luminance maps. After that, those approaches alter the reflectivity and luminance components and then recombine these to obtain the refined images. Fu et al. [6] presented a probabilistic method to better express prior information and estimate reflectivity and illumination. Guo [7] initially created a luminance map by identifying the highest intensity value for each of the pixels in the R, G and B channels. Afterwards, they introduced a skeleton prior to refining the initial illumination. Li et al. [1] improved the capability of enhancing underexposed pictures accompanied by rigorous noise. Ren et al. [8] incorporated lower ranking prior knowledge into a Retinex disaggregation procedure in order to reduce noise in the reflectivity map.

### 2.2 Learning-based Approaches

Learning-based approaches are dependent on paired underexposed and normal lighting pictures. Wei et al. [3] presented a deep learning structure, Retinex-Net, which combines a decomposition net for decomposition and an enhancement net for luminance adjustment. Jiang et al. [9] improved the contrast of the image by utilizing both its spatial and frequency information while also preserving its detailed characteristics. Zhang et al. [10] adopted a deep color coherence network to maintain the color consistency across LLIE. Cui et al. [11] proposed a framework in transformer style to evaluate ISP-related parameters to fuse the targeted images. Xu et al. [12] exploited Signal-to-Noise-Ratio-aware transformers and convolution filters to dynamically improve pixels. Wang et al. [13] presented a network framework that incorporates illumination-sensitive gamma correction and comprehensive image modeling. Yi et al. [14] integrated the strengths of the substantial model and the generative network to tackle various degradations.

Recently, unsupervised methods have been designed to minimize the overhead associated with gathering reference images. For example, Jiang et al. [15] presented a generative adversarial network that is pre-trained on non-paired pictures. Zhu et al. [16] devised a three-branch convolutive neural network for the purpose of conducting Retinex decomposition and restoration. Guo et al. [17] introduced a renewed approach for

estimating curves using deep learning techniques, without the need for any reference data. Liu et al. [18] presented a low-weight LLIE framework by merging the principled optimization Extending technique and incorporating a cooperative prior framework discovery tactic. Zhao et al. [19] implemented Retinex decomposition using deep neural networks to produce luminance and reflectivity maps, and the luminance map was then utilized to execute the enhancement process. Ma et al. [20] presented a cascaded illumination learning strategy with weight sharing to enhance poor images. They constructed the self-calibrated module to minimize calculation costs. Fu et al. [21] presented PairLIE, an unsupervised approach that leverages low-level lighting image pairs to learn adaptive priors.

### 3 Proposed Method

In Section 3.1, we will describe the process and steps of the presented method for enhancing underexposed images through a technique known as SDLLIE. Following that, in Section 3.2, we will delve into the specifics of the specially tailored loss function for SDLLIE, which is structured to facilitate zero-shot learning scenarios.

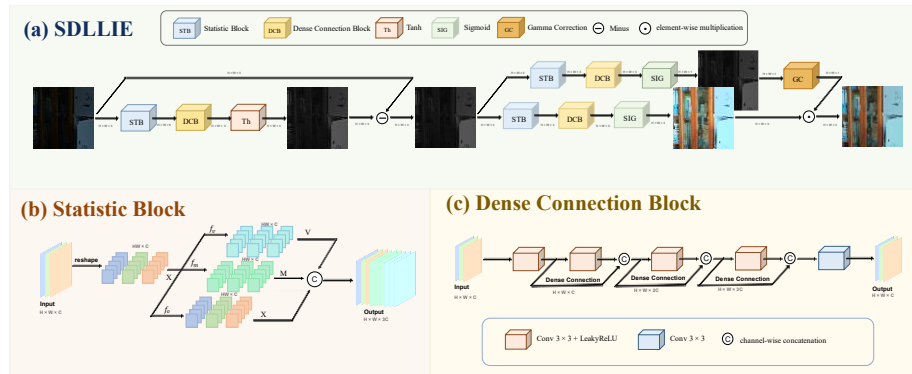


**Fig. 1.** The summarization of our method. (a) The SDLLIE consists of two components, denoising and restoring. (b) Statistic Blocks uses three branches to extract rich information from a single image. (c) Dense Connection Block consists of five convolutions and four LeakyReLU.

#### 3.1 Architecture of SDLLIE

On the basis of robust Retinex technology [1]. The disassembly of a low-light image  $I$  can be represented as the sum of a reflectance image  $R$ , an illumination image  $L$  and a noise map  $N$  as,

$$I = R \circ L + N \quad (1)$$

where  $\circ$  indicates the element by element multiplication. Fig. 1 displays the overall framework of our technique. As illustrated in Fig. 1 (a), Fig.1 (b) shows the specifics

of the Statistic Block. As indicated in Fig. 1 (c), the basic unit of the Dense Connection block, which is formed of five Convolution and four LeakyReLU.

**(1) Network:** In this network architecture, the decomposition processes resemble Retinex decomposition, but also have significant differences. During the feature extraction phase, the Statistic Block(STB) and Dense Connection Block(DCB) are used to extract information from low-light images. This ensures that all the rich information contained in the images is explored. The final step employs tanh and sigmoid activation functions to estimate noise, illumination maps, and reflection maps. However, the reflectance and illuminance branches terminate with a sigmoid layer to ensure that the intensities remain within the range of  $[0, 1]$ . Additionally, a tanh activation function is employed as the final layer of the noise branch to improve the accuracy of the noise map estimation, resulting in a decrease in noise values within the range of  $[-1, 1]$ . To minimize the impact of noise on the reflectance and illumination estimation of the low-light image, we use a comparatively clean low-level lighting image, denoted as  $I'$ , which is obtained by subtracting the noise from the original image  $I$ . The noise present in the image is represented by  $N$ , so that  $I' = I - N$ . During the training stage, the optimization process focuses on using the loss function to guide and constrain the decomposition process. This ensures that the model learns to accurately separate the image into its components. However, when transitioning to the testing stage, additional steps are introduced to further enhance the image. These steps typically involve performing gamma correction, as well as combining and refining the three key components: reflectance, illumination, and noise. By performing these post-processing procedures, the final output image undergoes further enhancement and adjustments, resulting in improved and visually appealing image quality:

$$I_e = G(L) \circ R = L^\gamma \circ R \quad (2)$$

where  $\gamma$  is the gamma correction factor and  $I_e$  means the enhanced picture.

**(2) Statistic Block:** Many LLIE techniques commonly utilize low-light images captured at different exposure levels as input to the network for enhancing details and improving image quality. However, the process of manual pre-selection of images based on prior knowledge is time-consuming and subjective, which can affect the quality of the generated results. Even with meticulous selection, there is no guarantee that the results will meet the desired standards of satisfaction. The Histogram Equalization (HE) method leverages the histogram to characterize the distribution of pixel intensity values in an image. By analyzing and adjusting the pixel distribution through histogram-based operations, the HE method aims to enhance the overall contrast and improve the visual quality of the image. Our approach is inspired by the principles of Histogram Equalization (HE) and leverages statistical analysis to extract valuable information from individual underexposed images. The method focuses on the raw pixel values, as well as their average and variance, to understand the distribution of pixel values across the image. By examining the relationship between pixel values and their spatial context, areas of potential improvement in exposure can be identified. In accordance with Fig. 1 (b), Initially, the input feature  $F$  is restructured into tokens  $X$ . Then  $X$  passes through three functions and is reconstructed:

$$X_g = F(f_o(X) + f_m(X) + f_v(X))_c \quad (3)$$

where  $X_g$  denotes the global information, and  $F_c$  means the concatenate operation. The result of  $F_o$  is the  $X$ .  $F_m$  and  $F_v$  indicate the mean and variance of the picture.

**(3) Dense Connection Block:** In convolutional neural networks, there is a tendency for global and contextual information to diminish as the network depth grows. While residual connections [22] can mitigate this issue, they may not be suitable for the LLIE task. Residual connections accumulate extracted features from the previous layer to the input of the next layer. This can lead to an increase in redundant information, which is not conducive to optimizing model parameters. To tackle this challenge, we consider increasing the network width. However, simply widening each layer may lead to model underfitting due to the limited number of datasets. Therefore, we draw inspiration from the benefits of dense connections [23], where each layer aggregates features from the previous layer, enabling richer information processing at each level. This approach not only mitigates network degradation but also facilitates the discovery of optimal model parameters during training. The conjecture can also be demonstrated in the ablation experiment section.

### 3.2 Loss function

In order to enhance the separation performance of the SDLLIE network, it is essential to update its parameters and design a criterion that measures the current separation performance. This criterion should guide the network to produce more precise individual elements. To achieve this, we have developed a loss function that considers various factors to evaluate the separation quality of the network. Below is a detailed explanation of the loss function design.

$$\mathcal{L} = \omega_1 \mathcal{L}_{rec} + \omega_2 \mathcal{L}_{inc} + \omega_3 \mathcal{L}_{rr} \quad (4)$$

where  $\mathcal{L}_{rec}$  is the reconstruction loss.  $\mathcal{L}_{inc}$  is the illumination-noise correlation loss.  $\mathcal{L}_{rr}$  is the reflectance reference loss.  $\omega_1$ ,  $\omega_2$ , and  $\omega_3$  are the hyper-parameters.

**(1) Reconstruction Loss:** To guarantee a dependable and precise decomposition, the extracted components from an image must conform to specific constraints that facilitate the reconstruction of the original image according to the specified equation Eq. (3). The objective of the reconstruction process is to minimize the difference between the reconstructed image and the original input image. Thus, the reconstruction loss can be expressed as a function that measures this difference and directs the optimization process to generate components that can accurately reconstruct the image. This loss function is essential in training the model to produce decomposed components that closely match the original image, resulting in high-quality and accurate reconstruction outcomes. The reconstruction loss can then be formulated as,

$$\mathcal{L}_{rec} = \|R \circ L + N - I\|_F \quad (5)$$

where  $R \circ L + N$  denotes the reconstructed image,  $I$  represents the input image and  $\|X\|_F$  refers to the Frobenius norm of the matrix  $X$ .

**(2) Illumination-Noise Correlation Loss:** During the process of enhancing low-level lighting images, the luminance of the dark portions is boosted to augment their clarity and perceptibility. However, this can also amplify any noise that may be present in those areas. Therefore, noise reduction is vital to prevent any unfavorable impact on subsequent enhancements. The luminance map reflects the brightness distribution of the picture, which can be applied to direct the task of image denoising and assist SDLLIE to estimate noise more efficiently in low-level lighting conditions. The term for the loss of correlation between illumination and noise has been designed accordingly.

$$\mathcal{L}_{inc} = \|L \circ N\|_2 + \frac{1}{n} \|L - L_m\|_2^2 + \alpha_1 \left\| \frac{\delta L}{\delta w} \right\|_1 + \alpha_2 \left\| \frac{\delta L}{\delta h} \right\|_1 \quad (6)$$

where  $\|X\|_2$  calculates the sum of squares of all the elements in  $X$ .  $\frac{1}{n} \|L - L_m\|_2^2$  is the mean absolute error (MSE) between  $L$  and  $L_m$ , the value of  $L_m$  is calculated by taking the maximum value from the R, G, and B channels.  $\|X\|_1$  denotes the summation of the absolute values of every element in  $X$ . Inspired by TVLoss [24], we propose two terms:  $\alpha_1 \left\| \frac{\delta L}{\delta w} \right\|_1$  and  $\alpha_2 \left\| \frac{\delta L}{\delta h} \right\|_1$ . The  $\alpha_1$  and  $\alpha_2$  represent the image dimensions, width and height, respectively.

**(3) Reflectance Reference Loss:** Supervised learning techniques use normal-light images as a reference during training to leverage the wealth of color information embedded in reflectance maps. We have formulated the reflectance reference loss as a crucial component in our training methodology, following the supervised approach of using reference images. The reflectance reference loss is used to compare and align predicted reflectance maps with corresponding reference images. This allows the model to learn and refine its predictions based on the desired output, resulting in accurate and consistent reflectance maps that closely resemble the reference images. The loss function enhances the quality and fidelity of the decomposition process. The reflectance reference loss can be expressed as:

$$\mathcal{L}_{rr} = \|R - R'\|_2^2 \quad (7)$$

where  $R'$  denotes the reflectance reference map, obtained by evaluating  $(I - N) / L$ . Based on signal processing principles, we assume that  $(I - N)$  represents a low-light image without noise.

## 4 Experiments

### 4.1 Datasets and Implementation Details

To evaluate the effectiveness of our suggested method for enhancing low-light images, we carried out comprehensive experiments on three publicly available datasets, including LOL-v1 [3], LOL-v2-real [25] and LOL-v2-synthetic [25]. The LOL-v1 dataset consists of 500 pairs of low/normal-light images, distributed into 485 training pairs and 15 testing pairs. The LOL-v2-real includes 689 pairs of low/normal-light images for

training and an incremental 100 pairs for testing. Similarly, the LOL-v2-synthetic datasets have 900 pairs of low/normal-light images for training and 100 pairs for testing. Only low-light images are used for training.

SDLLIE was implemented using PyTorch on a individual NVIDIA GTX 3090 GPU. During the training phase, a batch size of 16 is applied and images are randomly cropped to the size of  $48 \times 48$ . To optimize the network parameters, we employed the ADAM optimiser with an initial learning rate of  $1 \times 10^{-4}$ . For the training process, we established 600 epochs and implemented a learning rate reduction strategy where the rate was decreased by half every 100 epochs. Regarding the hyperparameters  $\omega_1$ ,  $\omega_2$ , and  $\omega_3$  in Equation 4, we empirically set  $\omega_1 = 70$ ,  $\omega_2 = 1.5$ , and  $\omega_3 = 1$ . In the testing stage. The default gamma correction factor  $\gamma$  is 0.15. The evaluation metrics employed are peak signal-to-noise ratio (PSNR), structural similarity (SSIM), mean absolute error (MAE) and learned perceptual image patch similarity (LPIPS).

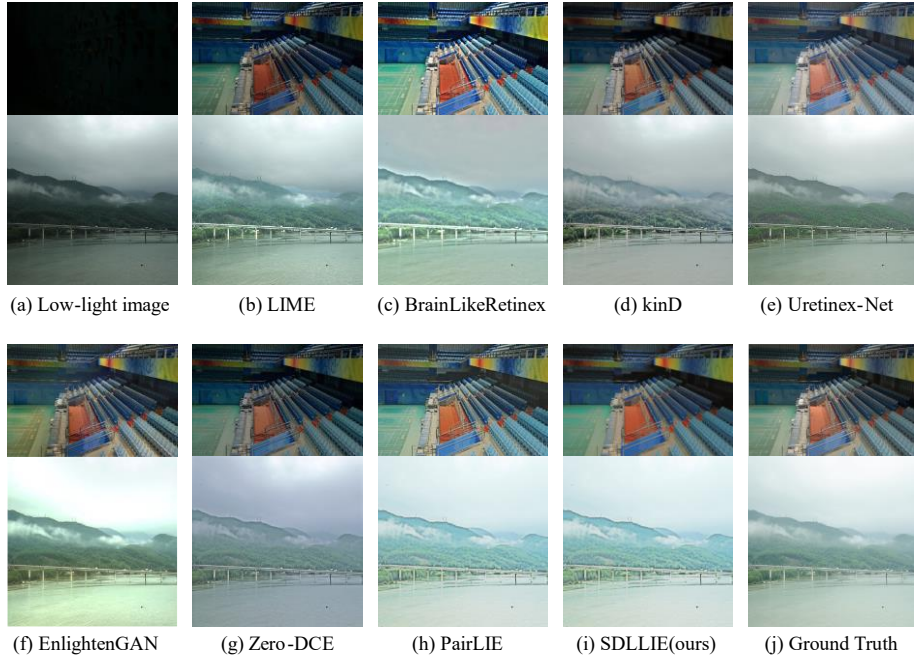


**Fig. 2.** Qualitative comparisons of different LLIE methods. LIME, BrainLikeRetinex, KinD, URetinex-Net, EnlightenGAN, Zero-DCE, PairLIE, and SDLLIE(ours).

## 4.2 Compared Methods

Thirteen state-of-the-art LLIE methods were compared with SDLLIE. These methods can be categorized into traditional, supervised, and unsupervised approaches. Those methods include LIME [7], Brain-Like Retinex [26], Retinex-Net [3], MBLLEN [27], KinD [29], ChebyLighter [2], URetinexNet [28], EnlightenGAN [15], RRDNet [16], Zero-DCE [17], RUAS [18], SCI [20], and PairLIE [21].



**Table 1.** Quantitative comparisons were made between the given method and state-of-the-art methods on the LOL-v1 and LOL-v2 datasets. "T", "S", and "U" correspond to the terms "Traditional", "Supervised", and "Unsupervised" approaches, respectively. In bold are the top three results.

Method	Type	LOL-v1				LOL-v2-real				LOL-v2-synthetic			
		PSNR $\uparrow$	SSIM $\uparrow$	MAE $\downarrow$	LPIPS $\downarrow$	PSNR $\uparrow$	SSIM $\uparrow$	MAE $\downarrow$	LPIPS $\downarrow$	PSNR $\uparrow$	SSIM $\uparrow$	MAE $\downarrow$	LPIPS $\downarrow$
LIME[11]	T	14.22	0.51	50.92	0.37	17.14	0.53	34.91	0.34	17.63	0.79	28.82	0.20
BrainLikeRetinex[3]	T	17.38	0.47	30.47	0.36	15.64	0.44	36.56	0.40	16.59	0.76	31.73	0.26
RetinexNet[34]	S	16.77	0.42	32.02	0.47	16.10	0.40	33.48	0.54	17.14	0.76	29.87	0.26
MBLLEN[23]	S	17.90	0.69	31.11	0.25	17.94	0.66	29.22	0.28	16.25	0.72	39.86	0.20
KimD[14]	S	17.65	<b>0.77</b>	31.40	<b>0.18</b>	<b>20.59</b>	<b>0.82</b>	<b>22.44</b>	<b>0.14</b>	17.28	0.76	33.18	0.25
ChebyLighter[12]	S	<b>19.74</b>	<b>0.75</b>	26.96	<b>0.20</b>	18.83	<b>0.77</b>	30.53	<b>0.18</b>	13.42	0.63	45.35	0.38
URetinexNet[47]	S	<b>21.33</b>	<b>0.83</b>	<b>21.17</b>	<b>0.12</b>	<b>21.22</b>	<b>0.86</b>	<b>23.17</b>	<b>0.10</b>	<b>18.76</b>	<b>0.83</b>	<b>27.44</b>	<b>0.19</b>
EnlightenGAN[30]	U	17.48	0.65	34.47	0.32	18.64	0.68	27.53	0.31	16.57	0.77	33.91	0.21
RRDNet[31]	U	11.40	0.46	69.83	0.36	13.90	0.48	53.36	0.32	14.79	0.65	45.96	0.25
Zero-DCE[32]	U	14.86	0.56	47.07	0.34	18.06	0.57	33.38	0.31	17.76	0.82	31.64	<b>0.17</b>
RUAS[33]	U	16.40	0.50	39.11	0.27	15.33	0.49	41.33	0.31	13.40	0.64	50.10	0.36
SCH[35]	U	14.78	0.52	48.76	0.34	17.30	0.53	37.49	0.31	15.43	0.75	39.85	0.23
PairLIE[36]	U	19.24	0.74	<b>26.04</b>	0.25	18.75	0.76	28.11	0.25	18.37	0.78	<b>28.40</b>	0.23
SDLLIE(ours)	U	<b>19.31</b>	<b>0.75</b>	<b>26.32</b>	0.34	<b>19.81</b>	0.69	<b>24.43</b>	0.35	<b>19.92</b>	<b>0.83</b>	<b>24.39</b>	<b>0.18</b>

### 4.3 Quantitative Comparisons

Tab. 1 shows the quantitative performance metrics for the LOL-v1, LOL-v2-real and LOL-v2-synthetic datasets. It is evident that traditional and unsupervised methods produce suboptimal results in these three datasets. This is due to the difficulty in learning optimal enhancement modeling parameters without reference images. Furthermore, some existing approaches depend on images with different exposure levels or manual priors, which can restrict their effectiveness and applicability in various scenarios. In many real-world situations, a more automated and robust solution is required as relying on carefully selected images or manual incorporation of prior knowledge may not be feasible or practical. SDLLIE achieves satisfactory performance compared to the other six unsupervised methods and gets comparable results among the supervised approaches in Tab. 1.

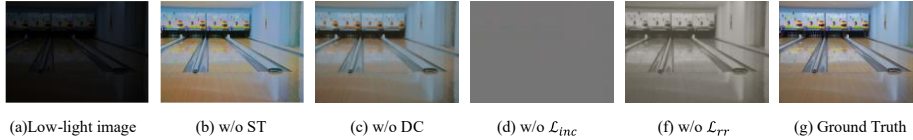
### 4.4 Qualitative Comparisons

Fig. 3 provides a visual comparison showcasing the quality outcomes of various Low-Light Image Enhancement (LLIE) methods on both the LOL-v2-real and LOL-v2-synthetic datasets. Analyzing the results in conjunction with Tab. 1, it becomes evident that the supervised methods KinD and URetinexNet exhibit commendable performance specifically on the LOL-v1 and LOL-v2-real datasets. However, our proposed approach demonstrates a well-rounded efficacy across all three benchmark datasets, with notable success observed on the LOL-v2-synthetic dataset. Notably, our method achieves compelling visual effects through the adept management of color rendering, contrast

enhancement, and preservation of natural tones, culminating in an overall enhancement of image quality and aesthetic appeal.

**Table 2.** Quantitative outcomes from the ablation research conducted on the LOL-v1 dataset. The optimal outcomes are emphasized in bold type.

Method	PSNR $\uparrow$	SSIM $\uparrow$	MAE $\downarrow$	LPIPS $\downarrow$
w/o STB	18.75	<b>0.75</b>	28.23	<b>0.32</b>
w/o DC	17.68	0.69	31.73	0.48
w/o inc	12.9	0.53	50.54	0.85
w/o rr	16.57	0.65	36.2	0.61
SDLLIE	<b>19.31</b>	0.75	<b>26.32</b>	0.34



**Fig. 3.** Qualitative comparisons of the ablation studies on the LOL-v1 dataset.

#### 4.5 Ablation Studies

Ablation studies were conducted on the LOL-v1 dataset to investigate the effectiveness of the proposed SDLLIE method in four experimental settings. The results of these studies are presented and analyzed in detail, providing valuable insights into the performance and impact of different components within the algorithm. The outcomes and findings of the ablation studies are presented in Tab. 2 for quantitative analysis and Fig. 2 for visual comparison. Upon the removal of  $\mathcal{L}_{inc}$ , a noticeable decline in performance is observed, leading to the generation of a grayscale output map. This outcome underscores the critical relationship between noise and illumination in the Low-light Image Enhancement process, highlighting the integral role that noise suppression plays in preserving image quality and enhancing visual clarity. The vibrancy and richness of color within the image can be significantly enhanced by incorporating  $\mathcal{L}_{rr}$ . By using this specific loss function, the enhancement algorithm is able to effectively enhance and amplify the color depth and saturation of the image, resulting in a visually striking and aesthetically pleasing output.  $\mathcal{L}_{rr}$  plays a pivotal role in fine-tuning the color representation and bringing out the vibrancy of the hues, contributing to an overall improvement in the visual appeal of the image. When dense connections are absent, the resulting image usually appears darker and less bright overall. Dense connections are essential for facilitating the flow of information and gradients throughout the network, ensuring that relevant features are effectively communicated and preserved across different layers. While the removal of STB may lead to a slight decrease in LPIPS values by a mere 0.02, it is important to note that this comes with a significant trade-off. Removing STB can result in overexposure in certain areas of the image, which can greatly compromise the overall quality and natural appearance of the enhanced image.

## 5 Conclusion

In this paper, we propose a general, reference-free approach, SDLLIE, which combines both Retinex-based and learning-based solutions to enhance low-light images. By introducing the overall change law of pixels, SDLLIE can extract more information from a single image and then better adapt to various scenarios. In order to better estimate the feature map, SDLLIE employs dense connections in the original convolution and then removes the noise map before estimating reflectance and illumination. Extensive quantitative and qualitative experiments show that SDLLIE outperforms the state-of-the-art unsupervised methods on public benchmarks. In the future, we will focus on exploring feature extraction methods for underexposed images.

## References

1. Li, M., Liu, J., Yang, W., Sun, X., & Guo, Z. Structure-revealing low-light image enhancement via robust retinex model. *IEEE Transactions on Image Processing*, 27(6), 2828-2841. (2018).
2. Pan, J., Zhai, D., Bai, Y., Jiang, J., Zhao, D., & Liu, X. ChebyLighter: Optimal Curve Estimation for Low-light Image Enhancement. In *Proceedings of the 30th ACM International Conference on Multimedia* (pp. 1358-1366). (2022, October).
3. Wei, C., Wang, W., Yang, W., & Liu, J. Deep retinex decomposition for low-light enhancement. *arXiv preprint arXiv:1808.04560*. (2018).
4. Abdullah-Al-Wadud, M., Kabir, M. H., Dewan, M. A. A., & Chae, O. A dynamic histogram equalization for image contrast enhancement. *IEEE transactions on consumer electronics*, 53(2), 593-600. (2007).
5. Celik, T., & Tjahjadi, T. Contextual and variational contrast enhancement. *IEEE Transactions on Image Processing*, 20(12), 3431-3441. (2011).
6. Fu, X., Liao, Y., Zeng, D., Huang, Y., Zhang, X. P., & Ding, X. A probabilistic method for image enhancement with simultaneous illumination and reflectance estimation. *IEEE Transactions on Image Processing*, 24(12), 4965-4977. (2015).
7. Guo, X. LIME: A method for low-light image enhancement. In *Proceedings of the 24th ACM international conference on Multimedia* (pp. 87-91). (2016, October).
8. Ren, X., Yang, W., Cheng, W. H., & Liu, J. LR3M: Robust low-light enhancement via low-rank regularized retinex model. *IEEE Transactions on Image Processing*, 29, 5862-5876. (2020).
9. Hai, J., Xuan, Z., Yang, R., Hao, Y., Zou, F., Lin, F., & Han, S. R2rnet: Low-light image enhancement via real-low to real-normal network. *Journal of Visual Communication and Image Representation*, 90, 103712. (2023).
10. Zhang, Z., Zheng, H., Hong, R., Xu, M., Yan, S., & Wang, M. Deep color consistent network for low-light image enhancement. In *Proceedings of the IEEE/CVF conference on computer vision and pattern recognition* (pp. 1899-1908). (2022).
11. Cui, Z., Li, K., Gu, L., Su, S., Gao, P., Jiang, Z., ... & Harada, T. You only need 90k parameters to adapt light: a light weight transformer for image enhancement and exposure correction. *arXiv preprint arXiv:2205.14871*. (2022).
12. Xu, X., Wang, R., Fu, C. W., & Jia, J. Snr-aware low-light image enhancement. In *Proceedings of the IEEE/CVF conference on computer vision and pattern recognition* (pp. 17714-17724). (2022).

13. Wang, Y., Liu, Z., Liu, J., Xu, S., & Liu, S. Low-light image enhancement with illumination-aware gamma correction and complete image modelling network. In *Proceedings of the IEEE/CVF International Conference on Computer Vision* (pp. 13128-13137). (2023).
14. Yi, X., Xu, H., Zhang, H., Tang, L., & Ma, J. Diff-retinex: Rethinking low-light image enhancement with a generative diffusion model. In *Proceedings of the IEEE/CVF International Conference on Computer Vision* (pp. 12302-12311). (2023).
15. Jiang, Y., Gong, X., Liu, D., Cheng, Y., Fang, C., Shen, X., ... & Wang, Z. Enlightengan: Deep light enhancement without paired supervision. *IEEE transactions on image processing*, 30, 2340-2349. (2021).
16. Zhu, A., Zhang, L., Shen, Y., Ma, Y., Zhao, S., & Zhou, Y. Zero-shot restoration of underexposed images via robust retinex decomposition. In *2020 IEEE International Conference on Multimedia and Expo (ICME)* (pp. 1-6). IEEE. (2020, July).
17. Guo, C., Li, C., Guo, J., Loy, C. C., Hou, J., Kwong, S., & Cong, R. Zero-reference deep curve estimation for low-light image enhancement. In *Proceedings of the IEEE/CVF conference on computer vision and pattern recognition* (pp. 1780-1789). (2020).
18. Liu, R., Ma, L., Zhang, J., Fan, X., & Luo, Z. Retinex-inspired unrolling with cooperative prior architecture search for low-light image enhancement. In *Proceedings of the IEEE/CVF conference on computer vision and pattern recognition* (pp. 10561-10570). (2021).
19. Zhao, Z., Xiong, B., Wang, L., Ou, Q., Yu, L., & Kuang, F. RetinexDIP: A unified deep framework for low-light image enhancement. *IEEE Transactions on Circuits and Systems for Video Technology*, 32(3), 1076-1088. (2021).
20. Ma, L., Ma, T., Liu, R., Fan, X., & Luo, Z. Toward fast, flexible, and robust low-light image enhancement. In *Proceedings of the IEEE/CVF conference on computer vision and pattern recognition* (pp. 5637-5646). (2022).
21. Fu, Z., Yang, Y., Tu, X., Huang, Y., Ding, X., & Ma, K. K. Learning a simple low-light image enhancer from paired low-light instances. In *Proceedings of the IEEE/CVF conference on computer vision and pattern recognition* (pp. 22252-22261). (2023).
22. He, K., Zhang, X., Ren, S., & Sun, J. Deep residual learning for image recognition. In *Proceedings of the IEEE conference on computer vision and pattern recognition* (pp. 770-778). (2016).
23. Huang, G., Liu, Z., Van Der Maaten, L., & Weinberger, K. Q. Densely connected convolutional networks. In *Proceedings of the IEEE conference on computer vision and pattern recognition* (pp. 4700-4708). (2017).
24. Rudin, L. I., Osher, S., & Fatemi, E. Nonlinear total variation based noise removal algorithms. *Physica D: nonlinear phenomena*, 60(1-4), 259-268. (1992).
25. Yang, W., Wang, W., Huang, H., Wang, S., & Liu, J. Sparse gradient regularized deep retinex network for robust low-light image enhancement. *IEEE Transactions on Image Processing*, 30, 2072-2086. (2021).
26. Cai, R., & Chen, Z. Brain-like retinex: A biologically plausible retinex algorithm for low light image enhancement. *Pattern Recognition*, 136, 109195. (2023).
27. Lv, F., Lu, F., Wu, J., & Lim, C. MBLLEN: Low-light image/video enhancement using CNNs. In *BMVC* (Vol. 220, No. 1, p. 4). (2018, September).
28. Wu, W., Weng, J., Zhang, P., Wang, X., Yang, W., & Jiang, J. Uretinex-net: Retinex-based deep unfolding network for low-light image enhancement. In *Proceedings of the IEEE/CVF conference on computer vision and pattern recognition* (pp. 5901-5910). (2022).
29. Zhang, Y., Zhang, J., & Guo, X. Kindling the darkness: A practical low-light image enhancer. In *Proceedings of the 27th ACM international conference on multimedia* (pp. 1632-1640). (2019, October).